

Oral and Maxillofacial Pathology

Expression of caspase-3 and structural changes associated with apoptotic cell death of keratinocytes in oral lichen planus

SI Tobón-Arroyave, FA Villegas-Acosta, SM Ruiz-Restrepo, B Vieco-Durán, M Restrepo-Misas, ML Londoño-López

Laboratorio de Inmunodetección y Bioanálisis, Facultad de Odontología, Universidad de Antioquia, Medellín, Colombia

OBJECTIVE: Apoptosis appears to be the mode of cell death by which damaged cells are removed from the lesional tissue. The aim of this study was to examine keratinocyte apoptosis and caspase-3 (CPP32) expression in oral lichen planus (OLP).

MATERIALS AND METHODS: Paraffin-embedded samples of OLP ($n = 30$) and normal oral mucosa (NOM; $n = 5$) were prepared for haematoxylin–eosin (H & E), immunohistochemistry and electron microscopy. The number of apoptotic cells and the proportion of total cells that were either apoptotic (apoptotic index; AI) or mitotic (mitotic index; MI) were assessed in H & E stained sections. An immunostaining-intensity-distribution index (IID; proportion of stained cells \times staining intensity) was used to assess CPP32 immunoreactivity.

RESULTS: Results showed a significant increase in the number of apoptotic cells in OLP ($P < 0.001$). In OLP, all apoptotic bodies were found in the basal and prickle epithelial layers. Compared with NOM, the AI was significantly greater in atrophic ($P < 0.05$), reticular ($P < 0.001$) and plaque-like ($P < 0.01$) OLP. The MI was significantly greater in plaque-like OLP ($P < 0.01$). The proportion of CPP32-positive cells and the IID were significantly greater in all forms of OLP compared with NOM ($P < 0.05$). No difference in CPP32 expression was evident between clinical forms of OLP. Electron microscopy confirmed the light microscopic finding of apoptosis.

CONCLUSION: Keratinocyte apoptosis and caspase-3 expression co-localized to the basal and parabasal epithelial layers, suggesting that proliferating epithelial cells may be targeted for destruction in OLP. Differences in epithelial AI and MI may underlie the various clinical and histological appearances of OLP.

Oral Diseases (2004) 10, 173–178

Keywords: apoptosis; CPP32; keratinocytes; oral lichen planus; ultrastructure

Introduction

Oral lichen planus (OLP) is a chronic mucosal disease with increased risk for malignant transformation (Silverman, 2000). Clinically it can present a confusing array of patterns and forms (Scully *et al*, 1998) but histological features are well described by WHO (Pindborg *et al*, 1997). Its diagnosis is based on the presence of an epithelial-connective tissue interface band of infiltrating T-lymphocytes (Sugerman *et al*, 2002). In OLP, basal epithelial cells undergo apoptotic changes, a process previously termed liquefaction degeneration (Bloor *et al*, 1999). It is assumed that these changes are due to the proximity of the sub-epithelial lymphocytic infiltrate (Villaruel-Dorrego *et al*, 2002).

Apoptosis is a tightly regulated process of genetically programmed cell death by which senescent, damaged and superfluous cells are eliminated from the body (Polverini and Nör, 1999) and it involves a series of histological changes, amongst these, nuclear shrinkage, chromatin condensation at the nuclear periphery, nucleolar disintegration and cytoplasm condensation (Kerr, Wyllie and Currie, 1972). Conventionally, apoptosis has been identified in preparations stained with haematoxylin–eosin (H & E) (Bloor *et al*, 1999). Furthermore to demonstrate the presence of apoptotic changes in OLP, immunohistochemical staining for apoptotic signalling proteins known as oncoproteins including bcl-2, bax, p21 and p53 has been performed (Dekker *et al*, 1997; Bloor *et al*, 1999; Tanda *et al*, 2000).

Caspases are cysteine-proteases of the interleukin-1 β -converting enzyme family, which are required for programmed cell death (Thornberry and Lazebnik, 1998). Many caspases participate in a cascade analogous to the coagulation system; upstream caspases cleave and

activate downstream caspases, which in turn cleave the various substrate proteins that account for many of the biochemical and morphological changes that occur during apoptosis (Patel, Gores and Kauffmann, 1996). Amongst these proteases, caspase-3 (CPP32) is the most downstream enzyme in the apoptosis-inducing protease pathway and is probably the most clearly associated with cell death (Woo *et al*, 1998) since it cleaves key proteins in the cell repairing process (Casciola-Rosen *et al*, 1996). CPP32 has been found in diverse normal tissues (Krajewska *et al*, 1997) and various studies have shown that its expression is related to the clinical outcome of several neoplasms (Donoghue *et al*, 1999; Kumamoto, Kimi and Ooya, 2001).

The purpose of this study was to evaluate the OLP cell death process by identifying changes in keratinocytes by means of H & E staining, immunohistochemical staining for CPP32 and transmission electron microscopy (TEM).

Materials and methods

Tissue samples

Biopsy material of buccal lichen planus was selected from laboratory archives, the diagnosis in each case having been made on the basis of clinical and histologic findings. All cases were assessed to reconfirm OLP diagnosis and to obtain clinical data. Those cases with previous history of habits (alcohol or tobacco), oral squamous cell carcinoma, oral-cervical-facial irradiation therapy, diabetes and hypertension were excluded from the study. Thirty cases ranging in age from 21 to 77 (mean 47.6) years with previously established criteria (Pindborg *et al*, 1997) were selected and three predominant OLP clinical forms were included: atrophic, reticular and plaque-like. As normal controls, five paraffin-embedded normal oral mucosa (NOM) samples of non-smoker patients ranging in age from 17 to 62 (mean 36) years were obtained. Two independent observers (ST & FV) performed blind specimen assessment, with an agreement of 95–97%, through use of an image analyzer system (AxioVision 3.1[®]; Carl Zeiss, Oberkochen, Germany).

Haematoxylin and eosin staining

About 4- μ m thick sections were mounted on silanized glass slides (Dako[®]; Dako Co., Carpinteria, CA, USA), H & E stained and observed using a Zeiss Axiolab[®] light microscope (Carl Zeiss, Oberkochen, Germany). Six high-power (400 \times magnification) fields were observed randomly on each slide, commencing with the first representative field on the left hand side of the section being counted, moving the stage to the next field and then continuing with measurement of alternative fields. Cells with apoptotic features were identified and analyzed based on previously defined criteria (Bloor *et al*, 1999). These included chromatin condensation at the periphery of the nucleus, uniformly eosinophilic cytoplasm, nuclear and/or cytoplasmic fragmentation, nuclear pyknosis, and nucleolar disintegration (classical bodies). Structures consisting of enlarged eosinophilic

bodies lacking nuclear material were categorized as colloid bodies. Apoptotic bodies consisting of small shrunken cells or hyaline residues without nuclear debris were classified as cytoplasmic bodies. The total number of cells, mitotic cells and the total of apoptotic bodies were recorded on each field. After counting the events, the number of apoptosis and mitoses, expressed as a percentage of observed cells [apoptotic index (AI), mitotic index (MI)] was recorded for each sample.

Immunohistochemistry

About 4- μ m thick sections were mounted on silanized glass slides (Dako[®]). Sections were deparaffinized in xylene, hydrated through graded alcohol and washed with phosphate buffered saline-PBS. Endogenous peroxidase activity was blocked with 3% H₂O₂ in methanol and endogenous biotin activity was quenched with Biotin Blocking System (Dako[®]) for 10 min. Antigen retrieval was performed by heating slides immersed in 10 mM citrate buffer (pH 6.0) in a microwave oven for 10 min. Sections were incubated with rabbit anti-human active CPP32 polyclonal antibody (Dako[®]) diluted 1:70. The standard streptavidin-biotin-peroxidase complex method was performed to bind the primary antibody with the use of a LSAB System Universal Kit (Dako[®]). Reaction products were visualized using 0.3% diaminobenzidine solution and counterstained with Harris haematoxylin. Paraffin-embedded B-cell lymphoma tissue was used as a positive control with known CPP32 expression. The specificity of immunohistochemical staining was determined by substituting the primary antibody with phosphate-buffered saline (PBS) or an irrelevant antibody of the same class (normal rabbit IgG).

Six high-power (400 \times magnification) fields were randomly chosen in each section. The cells with a clearly defined immunostaining as compared with the positive control were counted. The count was divided by the total number of cells in each field. The mean of the six fields was estimated for each sample. Furthermore each field was evaluated for the proportion of stained cells and the intensity of overall staining. The proportion of stained cells in each field was assessed as: 0, no stained cells; 1, <25% stained cells; 2, 25–50% stained cells; and 3, >50% stained cells. Staining intensity was graded as: 0, negative staining; 1, light staining; 2, moderate staining; and 3, intense staining. An immunostaining-intensity-distribution index (IIDI) was computed for each sample as follows: the score of the proportion of stained cells for each field was multiplied by the score of the staining intensity in that field to provide an IIDI for the field. The mean of the six fields was the IIDI for the sample.

Transmission electron microscopy

Samples were deparaffinized in xylene, hydrated in decreasing alcohol series and fixed in a Karnovsky solution (2.5% glutaraldehyde + 2.0% paraformaldehyde) diluted in a Sørensen phosphate buffer (pH 7.4; 0.1 M). They were post-fixed in 1% osmium tetroxide (OsO₄), dehydrated in increasing alcohol

series, infiltrated with propylene oxide and embedded in Spurr[®] resin (Taab Laboratories Ltd, Berkshire, UK). Ultra-thin sections (70 nm) were mounted on formvar-coated copper grids, post-stained with 4% uranyl acetate and lead citrate and examined using a Hitachi H-7000[®] electron microscope (Hitachi Co. Ltd, Tokyo, Japan). A descriptive analysis of the micrographs was performed.

Statistical analysis

Data were analyzed using SPSS 10.0[®] (SPSS Inc., Chicago, IL, USA) statistical package. Results were expressed as the mean ± s.d. To compare the number of apoptotic bodies, AI, MI, CPP32 expression estimation and the IIDI scores with respect to clinical forms, the non-parametric Mann–Whitney *U*-test was used. Correlations amongst AI and MI and between AI and CPP32 expression in each clinical form were assessed using Spearman’s rank correlation coefficient. Significance was established at a *P*-value < 0.05.

Results

Quantification of apoptosis by H & E

Apoptosis was not detected consistently in NOM by routine staining. Apoptotic cells and more frequently classical apoptotic bodies were observed along with intra-epithelial lymphocytes in all OLP sections, mainly in atrophic OLP (Table 1). The most common feature was rounded, convoluted cells, with uniformly eosinophilic cytoplasm and nuclear chromatin condensation (Figures 1 and 2). Cytoplasmic bodies in the form of small eosinophilic structures composed merely of cytoplasmic elements (Figure 1) and colloid bodies in the form of large eosinophilic structures devoid of nuclear material (Figure 2), although observed in all OLP forms, were less frequent. All apoptotic bodies were found in the basal and prickle epithelial layers. A significant statistical difference was observed (*P* < 0.001) in the total of apoptotic bodies between each OLP form and the NOM samples. The results of apoptotic and mitotic indexes are shown in Table 2. A significant statistically difference between AI values in each OLP form and NOM was observed, whilst a significant difference was only observed between MI values in plaque-like OLP and NOM. Both AI and MI had their maximum value in plaque-like OLP. A weak and no significant correlation (*r* = 0.24, *P* = 0.165) between AI and MI was observed.

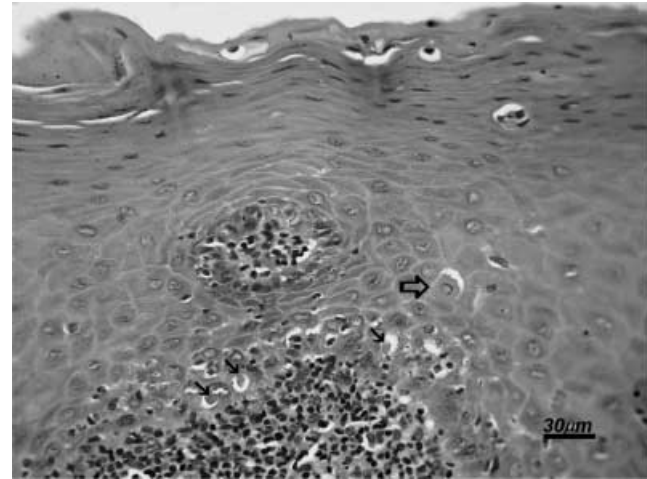


Figure 1 Oral lichen planus light microphotograph showing several cytoplasmic bodies (thin arrows) along basal cell zone and a classical apoptotic body (thick arrow) in the prickle layer (H&E, original magnification 400×)

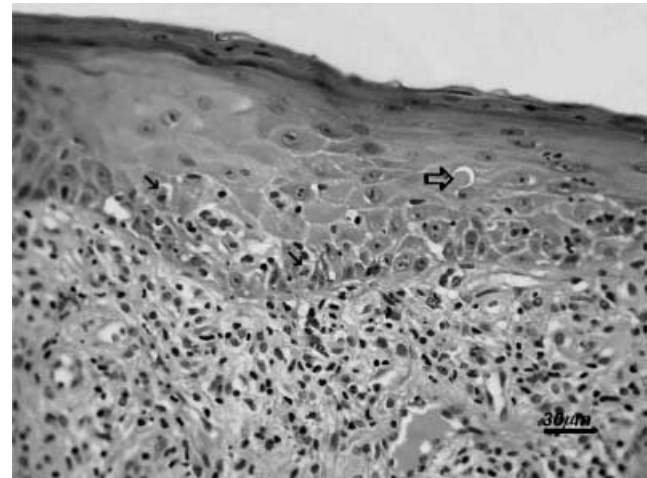


Figure 2 Oral lichen planus light microphotograph showing a colloid body (thick arrow). Synchronously two classical bodies (thin arrows) are also seen in the basal cell layer (H&E, original magnification 400×)

Detection of CPP32

Immunoreactivity for CPP32 was found in the cytoplasm and often in the nuclei of both normal and pathological keratinocytes. Its expression was stronger

Table 1 Mean number of apoptoses per high-power field in NOM and OLP identified by H & E staining

Clinical groups	Number of fields	Mean of apoptotic bodies (±s.d.)				<i>P</i> -value ^a
		Classical	Cytoplasmic	Colloid	Total	
NOM	30	–	–	0.03 ± 0.18	0.03 ± 0.18	
Atrophic	42	0.83 ± 1.17	0.19 ± 0.55	0.12 ± 0.50	1.12 ± 1.63	<0.001
Reticular	66	0.48 ± 0.98	0.27 ± 0.51	0.14 ± 0.39	0.89 ± 1.45	<0.001
Plaque-like	72	0.51 ± 0.93	0.24 ± 0.54	0.17 ± 0.50	0.92 ± 1.29	<0.001

^aMann–Whitney *U*-test.

Table 2 Apoptotic index (AI) and mitotic index (MI) assessed by H & E staining

Clinical groups	Number of cases	Apoptotic index		Mitotic index	
		Mean ± s.d.	P-value ^a	Mean ± s.d.	P-value ^a
NOM	5	0.02 ± 0.04		0.09 ± 0.11	
Atrophic	7	0.73 ± 0.76	0.018	0.17 ± 0.12	0.343
Reticular	11	0.66 ± 0.61	<0.001	0.26 ± 0.27	0.221
Plaque-like	12	0.82 ± 1.33	0.009	0.34 ± 0.19	0.006
P-value ^b			0.165		

^aMann-Whitney *U*-test, compared with normal oral mucosa (NOM).

^bSpearman's rank correlation coefficient.

in basal and parabasal layers and weak in the prickle layer (Figure 3a). Most of lymphocytes in the subepithelial and intraepithelial infiltrate also presented an intense staining. NOM tissues exhibited weak immunoreactivity with a homogeneous distribution in the basal and parabasal layers (Figure 3b). A significant

difference was observed in CPP32 expression between each form of OLP and NOM (Table 3). The IIDI score was significantly higher in each form of OLP than the score in NOM (Table 4). No significant difference was observed for CPP32 expression nor the IIDI score between the clinical forms of OLP. The comparison of the CPP32 expression and AI showed no significant correlation within the clinical groups (data not shown). In all immunohistochemical control experiments where antibody was omitted or where irrelevant antibodies of the same class were used, there was complete absence of staining (Figure 3c). Positive control tissue showed strong reactivity (Figure 3d).

Ultrastructural findings

Cells with early apoptotic changes characterized by compaction and segregation of chromatin in electron-dense circumscribed uniformly granular masses; convolution of the nuclear outline and condensation of the cytoplasm with relative preservation of the cell structure (Figure 4a) were observed. A common feature was the

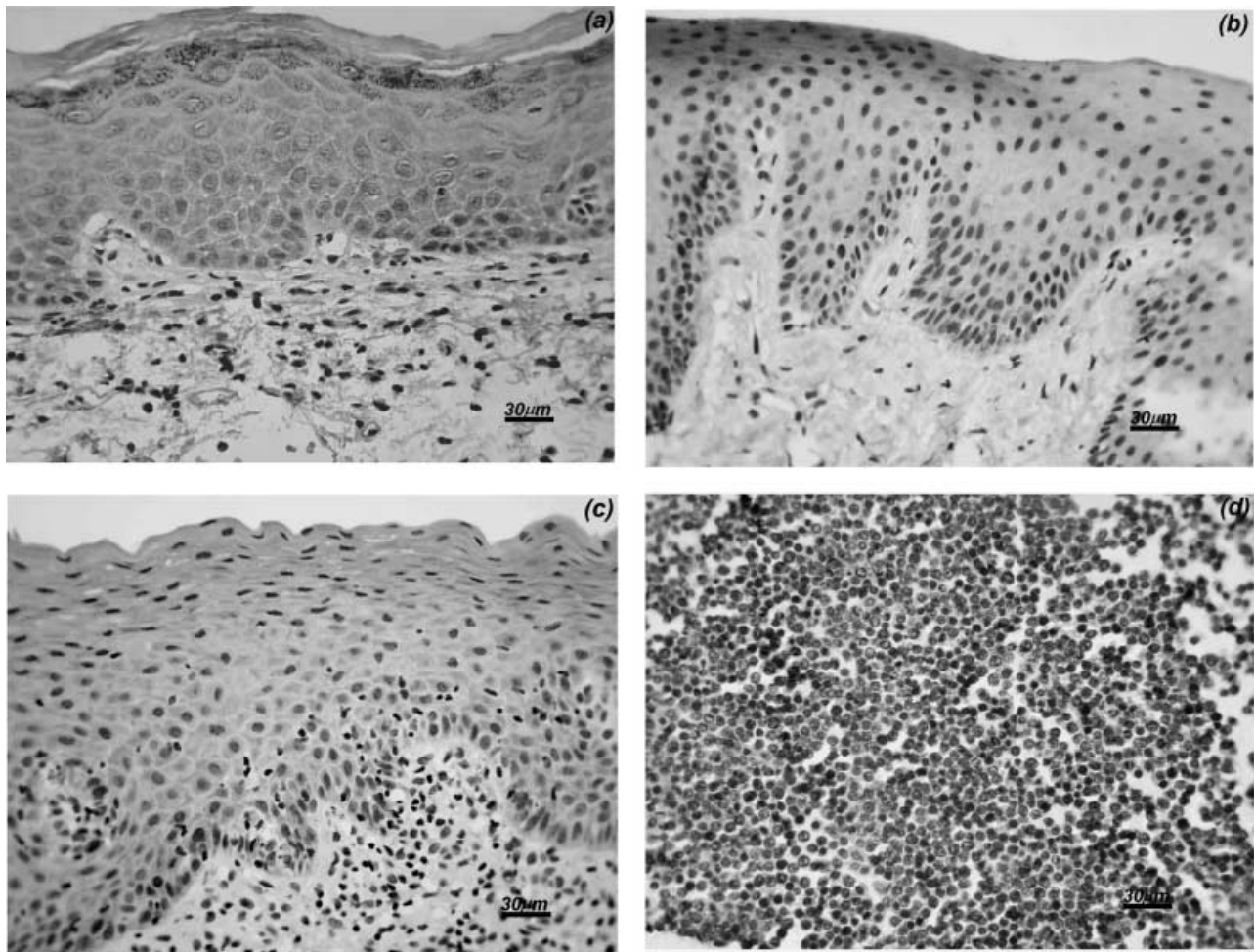


Figure 3 Immunohistochemical reactivity for active caspase-3. (a) Expression of CPP32 in oral lichen planus. Numerous basal and prickle cells show a weak to moderate staining. (b) NOM tissue showing weak immunoreactivity with a homogeneous distribution in the basal and parabasal layers. (c) Negative control with isotype matched staining. Note complete absence of staining. (d) Positive control showing cytoplasmic staining of lymphoid cells (haematoxylin counterstain, original magnification 400x)

Table 3 CPP32 expression estimation in NOM and OLP specimens (mean ± s.d.)

Clinical groups	Number of cases	CPP32 expression (stained cells/total cell number)	P-value ^a
NOM	5	0.51 ± 0.30	
Atrophic	7	0.87 ± 0.12	0.010
Reticular	11	0.83 ± 0.23	0.027
Plaque-like	12	0.84 ± 0.14	0.014

^aMann–Whitney U-test.

Table 4 Immunostaining–intensity–distribution index (IIDI) scores for CPP32 expression in NOM and OLP specimens (mean ± s.d.)

Clinical groups	Number of cases	IIDI score	P-value ^a
NOM	5	2.37 ± 1.46	
Atrophic	7	6.64 ± 1.35	0.003
Reticular	11	5.94 ± 2.56	0.013
Plaque-like	12	5.21 ± 2.07	0.006

^aMann–Whitney U-test.

presence of electron-dense bodies composed mainly of condensed nuclear chromatin (Figure 4b). Apoptotic lymphocytes with scant cytoplasm, convoluted nuclei and chromatin margination in clusters bounded to the nuclear periphery were also observed in close association with the epithelial cells (Figure 4c). These were different to those observed in the stroma, which showed a large ovoid nucleus with a higher and dispersed chromatin concentration.

Discussion

This study confirmed that different morphological types of the apoptotic phenotype are prevalent in OLP. Cell depletion by apoptosis must be compensated by means of cell division to keep the constant epithelial tissue thickness (Bloor *et al*, 1999). This would explain the clinical behaviour of the three types of OLP analyzed, because the plaque-like lesions had significantly higher values for AI and MI. On the other hand, MI was much lower in the atrophic forms and intermediate in the reticular forms reflecting the thickness loss resulting from an increased AI.

The presence of intra-epithelial lymphocytes in OLP has been previously described (Walton *et al*, 1998). In this study intra-epithelial lymphocytes observed by TEM, showed apoptotic changes and were in close association with keratinocytes. It has been shown that as disease progress there is a gradual accumulation of CD8+ T-cells within the epithelium (Villarreal-Dorrego *et al*, 2002). Once within the epithelium, CD8+ lymphocytes secrete granzyme B around keratinocytes triggering nuclear injury (Shimizu *et al*, 1997). *In vitro* assays have shown the capability of granzyme B to cleave and activate CPP32 (Quan *et al*, 1996) which might initiate a chain of events that takes the epithelial cells irreversibly to apoptosis. It is probable that there is also CPP32 self-activation in T-cells, which would explain the presence of apoptotic lymphocytes.

It has been found that CPP32 expression in normal tissues differs according to the cell type and differentiation stage (Krajewska *et al*, 1997). In this study, CPP32 was strongly expressed by basal epithelial cells, suggesting that the caspase cascade is active within the proliferating compartment in OLP epithelium in contrast

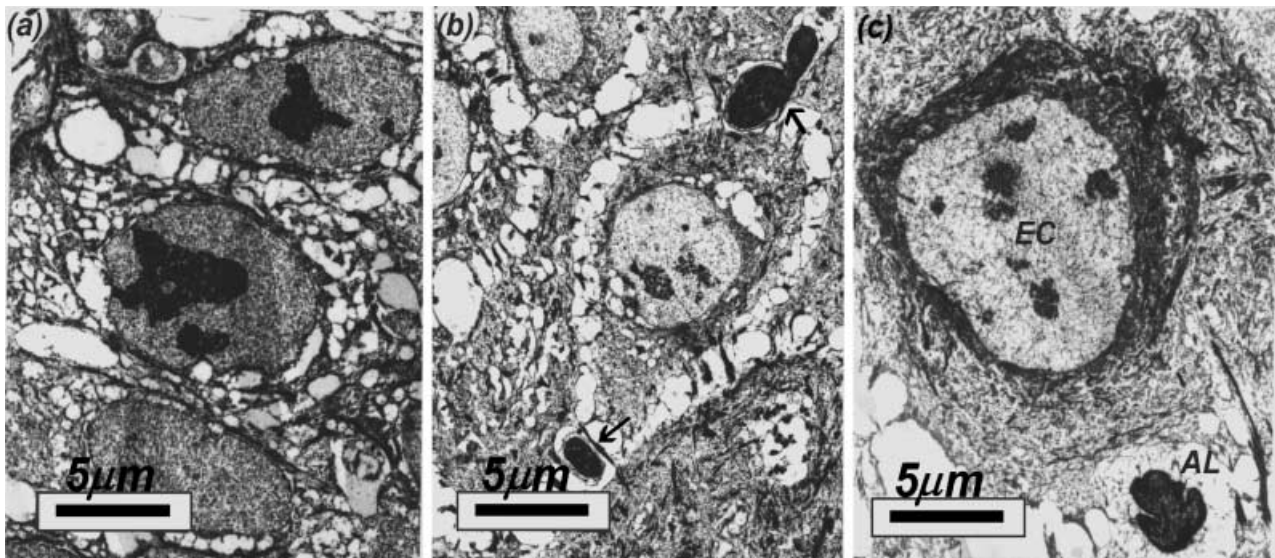


Figure 4 Oral lichen planus electron micrographs showing different changes of apoptosis. (a) Note shrinkage of the nuclear membrane and chromatin segregation condensed into circumscribed, electrondense, granular masses. (b) Apoptotic fragments (arrows) exclusively compound of dense granular nuclear chromatin. (c) Apoptotic lymphocyte (AL) with scant cytoplasm, convoluted nucleus and chromatin margination against the nuclear periphery associated to an epithelial cell (EC) with perinuclear tonofibrils disposed in a spiral array (lead citrate-uranyl acetate, original magnification 3000×)

with NOM samples where CPP32 immunoreactivity was essentially weak. Little is known about CPP32 expression in oral pathological conditions (Kumamoto *et al*, 2001). In this study, the CPP32 over-expression and the significant differences in the IIDI in OLP as compared with the controls could indicate the involvement of this cytosolic protease in the pathogenesis of the disease. CPP32 expression in the prickle cell layer was similar in OLP and NOM, suggesting a role for caspase-3 in keratinocyte differentiation in both normal and diseased oral mucosa (Krajewska *et al*, 1997). Furthermore, many sub- and intraepithelial lymphocytes also were positive, indicating their apoptotic activity. CPP32 expression is correlated with the differential ability to undergo apoptosis in tissues *in vivo*, including epidermis (Krajewska *et al*, 1997). In this study, despite of finding higher values for AI and CPP32 expression, no statistically significant correlation between them was observed. It is probable that the observed differences in the three OLP types suggest that the CPP32 expression can be up-regulated along with an increased vulnerability of keratinocytes to apoptosis. Proteolytic activation of CPP32 can be modulated by the suppressing oncoprotein family bcl-2 (Monney *et al*, 1996; Chang and Yang, 2000). On this basis, the lack of expression of bcl-2 observed in OLP (Dekker *et al*, 1997; Bloor *et al*, 1999) could make keratinocyte cell death possible through a caspase cascade activation. Furthermore, p53 expression in the basal and suprabasal keratinocytes in OLP (Dekker *et al*, 1997) could be related to the caspase pathway (Chang and Yang, 2000). It has been stated that p53 stimulates the transcription of Bax (Miyashita and Reed, 1995); Bax blocks the activity of bcl-2 (Oltvai, Milliman and Korsmeyer, 1993); bcl-2 normally blocks the activation of caspase-3 (Monney *et al*, 1996). When bcl-2 activity is blocked by Bax, caspase-3 activity is unchecked and apoptotic cell death proceeds. p53 also represses the transcription of bcl-2 (Miyashita *et al*, 1994) which further contributes to caspase-3 activity and apoptosis.

In conclusion, apoptosis in OLP was identified by light and electron microscopy. Keratinocyte apoptosis and caspase-3 expression co-localized to the basal and parabasal epithelial layers, suggesting that proliferating epithelial cells may be targeted for destruction in OLP. Differences in epithelial AI and MI may underlie the various clinical and histological appearances of OLP.

References

Bloor B, Malik F, Odell E *et al* (1999). Quantitative assessment of apoptosis in oral lichen planus. *Oral Surg Oral Med Oral Pathol Oral Radiol Endod* **88**: 187–195.

Casciola-Rosen L, Nicholson DW, Chong T *et al* (1996). Apopain/CPP32 cleaves proteins that are essential for cellular repair: a fundamental principle of apoptotic death. *J Exp Med* **183**: 1957–1964.

Chang H, Yang X (2000). Proteases for cell suicide: functions and regulation of caspases. *Microbiol Mol Biol Rev* **64**: 821–846.

Dekker NP, Lozada-Nur F, Lagenaur LA *et al* (1997). Apoptosis-associated markers in oral lichen planus. *J Oral Pathol Med* **26**: 170–175.

Donoghue S, Baden HS, Lauder I *et al* (1999). Immunohistochemical localization of caspase-3 correlates with clinical outcome in B-cell diffuse large-cell lymphoma. *Cancer Res* **59**: 5386–5391.

Kerr J, Wyllie AH, Currie AR (1972). Apoptosis: a basic biological phenomenon with wide-ranging implications in tissue kinetics. *Br J Cancer* **26**: 239–257.

Krajewska M, Wang H-G, Krajewski S *et al* (1997). Immunohistochemical analysis of *in vivo* patterns of expression of CPP32 (caspase-3), a cell death protease. *Cancer Res* **57**: 1605–1613.

Kumamoto H, Kimi K, Ooya K (2001). Immunohistochemical analysis of apoptosis-related factors (Fas, Fas ligand, caspase-3 and single-stranded DNA) in ameloblastomas. *J Oral Pathol Med* **30**: 596–602.

Miyashita T, Reed JC (1995). Tumor suppressor p53 is a direct transcriptional activator of the human bax gene. *Cell* **80**: 293–299.

Miyashita T, Krajewski S, Krajewska M *et al* (1994). Tumor suppressor p53 is a regulator of bcl-2 and bax gene expression *in vitro* and *in vivo*. *Oncogene* **9**: 1799–1805.

Monney L, Otter I, Olivier R *et al* (1996). Bcl-2 overexpression blocks activation of the death protease CPP32/YAMA/apopain. *Biochem Biophys Res Commun* **221**: 340–345.

Oltvai ZN, Milliman CL, Korsmeyer SJ (1993). Bcl-2 heterodimerizes *in vivo* with a conserved homolog, Bax, that accelerates programmed cell death. *Cell* **74**: 609–619.

Patel T, Gores GJ, Kauffmann SH (1996). The role of proteases during apoptosis. *FASEB J* **10**: 587–597.

Pindborg JJ, Reichart PA, Smith CJ *et al* (1997). *Histological typing of cancer and precancer of the oral mucosa*. World Health Organisation International Classification of Tumours. Springer-Verlag: Berlin. p 30.

Polverini PJ, Nör JE (1999). Apoptosis and predisposition to oral cancer. *Crit Rev Oral Biol Med* **10**: 139–152.

Quan L, Tewari M, O'Rourke K *et al* (1996). Proteolytic activation of cell death protease YAMA/CPP32 by granzyme B. *Proc Natl Acad Sci USA* **93**: 1972–1976.

Scully C, Beyli M, Ferreiro MC *et al* (1998). Update on oral lichen planus: etiopathogenesis and management. *Crit Rev Oral Biol Med* **9**: 86–122.

Shimizu M, Higaki Y, Higaki M *et al* (1997). The role of granzyme B-expressing CD8-positive T cells in apoptosis of keratinocytes in lichen planus. *Arch Dermatol Res* **289**: 527–532.

Silverman S (2000). Oral lichen planus: a potentially premalignant lesion. *J Oral Maxillofac Surg* **58**: 1286–1288.

Sugerman PB, Savage NW, Walsh LJ *et al* (2002). The pathogenesis of oral lichen planus. *Crit Rev Oral Biol Med* **13**: 350–365.

Tanda N, Mori S, Saito K *et al* (2000). Expression of apoptotic signalling proteins in leukoplakia and oral lichen planus: quantitative and topographical studies. *J Oral Pathol Med* **29**: 385–393.

Thornberry NA, Lazebnik Y (1998). Caspases: enemies within. *Science* **281**: 1312–1316.

Villarreal-Dorrego M, Correnti M, Delgado R *et al* (2002). Oral lichen planus: immunohistology of mucosal lesions. *J Oral Pathol Med* **31**: 410–414.

Walton LJ, Macey MG, Thornhill MH *et al* (1998). Intraepithelial subpopulations of T lymphocytes and Langerhans cells in oral lichen planus. *J Oral Pathol Med* **27**: 116–123.

Woo M, Hakem R, Soengas MS *et al* (1998). Essential contribution of caspase 3/CPP32 to apoptosis and its associated nuclear changes. *Genes Dev* **12**: 806–819.

Copyright of Oral Diseases is the property of Blackwell Publishing Limited and its content may not be copied or emailed to multiple sites or posted to a listserv without the copyright holder's express written permission. However, users may print, download, or email articles for individual use.